Digitally Tunable Microfluidic Optical Fiber Devices

Francesco Cattaneo, Kirk Baldwin, Shu Yang, Tom Krupenkine, Siddharth Ramachandran, and John A. Rogers

***Abstract*—This communication introduces a digital design for tunable microfluidic optical fiber devices. In these systems, multiple, independently controlled microfluidic plugs are pumped into or out of overlap with a fiber structure to modulate its transmission characteristics. The devices described here use eight plugs, eight electrowetting pumps and a corresponding set of molded planar recirculating microchannels to control the depth of the narrow-band loss feature associated with a long period fiber grating. Optical measurements illustrate the digital and relatively fast operation of this type of microfluidic fiber device. [991]**

***Index Terms*—Fluidics, microfluidics, micropumps, optical device fabrication, optical fiber applications, optical fiber devices.**

I. Introduction

TUNABLE optical fiber devices are attractive for many important operations in optical communication systems—dynamic chromatic dispersion compensation, programmable adding and dropping of wavelength channels, dynamic gain equalization, etc. These devices naturally incorporate the beneficial attributes of optical fiber (i.e., low cost, polarization independent behavior, etc.) together with the well-developed techniques for fiber manipulation (i.e., splicing, terminating, etc.). They also avoid many of the disadvantages—difficult alignment tolerances, challenging reliability requirements, optical coupling difficulties, etc.—of more traditional components that use bulk optics, waveguides or conventional microelectromechanical systems, and which requires light to be coupled out of and back into the fiber. Existing tunable fiber devices rely almost exclusively on simple thermo-optic and strain-optic effects. The recent introduction of pumped microfluidics into the area of fiber optics provides a new class of component with broad and flexible tuning characteristics [1]–[4]. This type of photonic component, known as microfluidic optical fiber (μFF), can provide attractive features—low power, nonmechanical operation, wide tuning range, low insertion loss, polarization independent behavior, etc.—that could make them useful for certain applications in optical networking. Two μFF designs have been explored so far. One uses integrated thermal micropumps and actuators to control the positions and optical properties of microfluidic plugs in the channels of specially designed "holey" fibers [1], [3]. When combined with in-fiber gratings or fiber tapers, this type of tunable microfluidic fiber can form the basis of wavelength and depth adjustable narrow-band filters [1], variable broadband attenuators [3], and other devices. In another μFF design, electrowetting pumps and planar microfluidic channels are used with conventional fiber to yield components that can offer similar functionality but with improved optical characteristics [2], [4]. This design also benefits from the ability of the electrowetting pumps to provide relatively fast switching and power efficient, latchable operation. In both cases, the microfluidic plugs move back and forth along a length of fiber whose optical properties are sensitive to the presence of the fluid. The plug velocity and the distance that the plugs must travel in order to overlap completely the relevant fiber structure determine the switching speed. For devices that use long period fiber gratings, this distance is equal to the length of the grating, which is typically a few centimeters. Corresponding switching times are typically on the order of one second for plug velocities that can be easily achieved with electrowetting or thermal pumps. For many (but not all) applications, this speed might not be sufficient. Another disadvantage of the previous designs is that the plug position is difficult to control precisely without active feedback. As a result, reproducibly and quickly achieving desired tuning states can be challenging when the system is operated in open loop. This axial pumping geometry also only allows various states of overlap of a single fluid plug starting at one end of the fiber structure. It is not possible, for example, to achieve variable overlap lengths in the center region of a fiber grating, or multiple overlaps at different locations along the fiber, both of which are useful capabilities that could enable tunable microfluidic phase shifted or sampled gratings, and other types of devices.

This communication describes an electrowetting-based microfluidic design that overcomes many of the disadvantages of the previous systems. It uses multiple, independently controlled microfluidic plugs that are side-pumped into or out of overlap with a conventional optical fiber. This system offers a digital form of microfluidic tuning: each plug in the device is either in overlap with the fiber or it is not. Repeatable tuning to desired levels does not require feedback, and a given tuning state is stable over long periods of time without any form of active control. In addition, switching can be fast since the distance that the plugs must move in order to overlap the fiber is comparable to the diameter of the fiber; it is independent of the length of the fiber structure that is switched. This paper starts with a description of the design and fabrication of this type of fluidic system. It illustrates the good optical performance that is possible and some of the benefits of digital operation when implemented with a conventional long-period fiber grating (LPG) [5]. Cascaded arrays of these types of components can be used to achieve complex tunable filters that can be used for dynamic gain equalization and other applications in optical networking.

Manuscript received January 16, 2003; revised June 24, 2003. The work of F. Cattaneo was supported by Fondazione Banca del Monte di Lombardia, Milan, Italy, and Collegio Ghislieri, Pavia, Italy. Subject Editor N. C. Tien.

F. Cattaneo, K. Baldwin, S. Yang, and T. Krupenkine are with the Bell Laboratories, Lucent Technologies, Murray Hill, NJ 07974 USA.

S. Ramachandran is with the OFS/Fitel, Murray Hill, NJ 07974 USA.

J. A. Rogers is with the University of Illinois at Urbana/Champaign, Urbana, IL 61801 USA (e-mail: jrogers@uiuc.edu).

Digital Object Identifier 10.1109/JMEMS.2003.820285

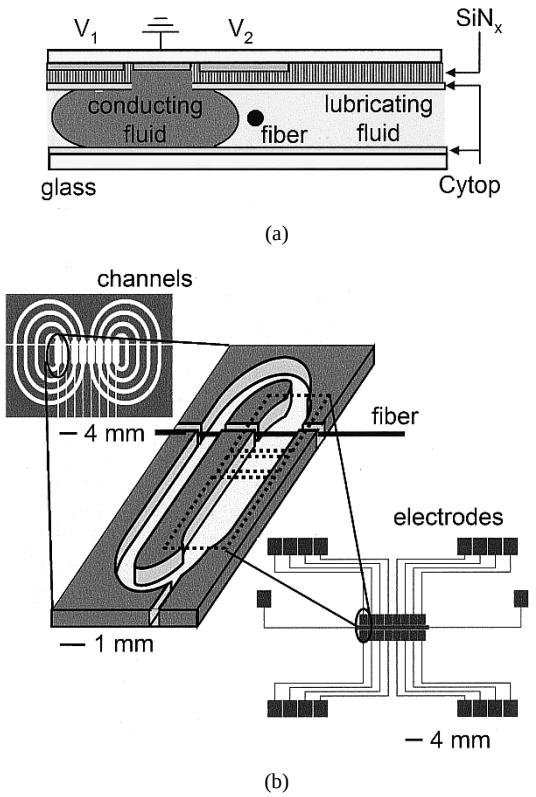

Fig. 1. Part (a) shows a cross-sectional schematic side view of a microfluidic cell with an electrowetting pump. A conductive fluid is contained between two substrates: one that supports channels that define the microfluidic network (bottom substrate) and one that supports the electrodes for the electrowetting pumps (top substrate). A 'via' hole electrically connects the conducting plugs to a common ground electrode. The pump is designed to move the plugs into or out of overlap with the fiber (end on view, shown on the right). Part (b) shows the layout of the two substrates and an angled view that illustrates how these elements are arranged. The top left (light areas represent the fluid channels) and bottom right (dark areas represent the electrodes) insets show the overall layout of a system that uses eight independently controlled fluid plugs. Each plug is housed in a recirculating channel designed to avoid flow-induced backpressure.

II. Experimental

A. Design and Operation of the Microfluidic System

The microfluidic system consists of eight independently controlled fluid plugs that can be pumped, using an electrowetting technique, into or out of overlap with short segments of an optical fiber (see Fig. 1). It involves two separate parts that are brought together to form the fluidic component of the device: one substrate that supports the microchannel structure and a different substrate that supports the electrodes and dielectric layers which provide the corresponding array of electrowetting pumps. The channels provide eight independent recirculating "racetracks" designed so that plug motion does not generate unwanted backpressure, which can inhibit flow. This layout also allows the entire device to be hermetically sealed, without affecting the fluid flow. The fiber rests in a slot that is perpendicular to and passes through the straight sections of these recirculating racetrack channels. The channels widen near the location of the fiber, to provide some physical confinement of the conducting fluid near the fiber. Conducting fluid plugs are injected into these wide regions using micropipettes threaded through narrow channels that lead to these regions. The fluid consists of an aqueous solution of $Na_2Cr_2O_7 \cdot 2H_2O$ with a concentration ($\sim 58\%$ by weight) that yields an index of refraction closely matched to the fiber cladding at wavelengths near 1.5 μm. The entire system is backfilled with a low viscosity, low surface energy silicone fluid (DMSS-T00; Gelest) to lubricate flow of these plugs.

The substrate that supports the electrowetting pumps rests on top of the fluid filled channels. This element consists of an array of electrodes that are patterned to overlap with the wide regions of the channels near the fiber. There are three separate electrodes in each region. One of these, which electrically connects all of the conducting plugs, provides a common ground. There are two other electrodes for each plug: one that overlaps the edge of the plug nearest the fiber, and one that overlaps the other edge. A dielectric coating prevents direct electrical contact. By applying suitable voltages to these electrodes, it is possible, through the electrowetting effect [6], to control independently the contact angles at each end of each one of the eight plugs. In particular, the electric field that is produced between the conductive fluid and the underlying electrode leads to the accumulation of charge at the fluid-dielectric and dielectric-electrode interfaces in a manner analogous to a simple parallel-plate capacitor. The energy cost associated with the liquid covering the dielectric is consequently reduced in direct proportion to the capacitive energy developed upon field application. If the liquid on the dielectric substrate is initially "nonwetting," then the effect of the field is to reduce the contact angle in direct proportion to the square of the applied voltage. Contact angle differences between the two ends of any given plug (which are proportional to the square of the difference between the applied voltages [6]) provides a driving force that pumps the plug toward the electrode that is held at the higher voltage, at velocities of a few centimeters per second. The control electrodes are patterned such that they terminate at short distances away from the fiber. As a result, when a voltage is applied to an electrode, the corresponding plug moves rapidly until it encounters the electrode edge. At this point, there is no electrowetting force to drive continued motion of the plug, so it abruptly stops. These patterned electrodes therefore provide virtual damns that naturally prevent the plugs from moving beyond positions that are just in or out of overlap with the fiber. Maintaining the voltage on the electrode actively holds the plug in its final position. This feature is important for the robust, digital operation of the device.

Fig. 1(a) gives a schematic cross sectional view of one of the eight plugs and its relationship to the fiber and other elements of the device. Part (b) of this figure presents a schematic angled view of one of the recirculating channels. The insets on the top left (light regions represent the channels) and bottom right (dark regions represent the electrodes) of Fig. 1(b) show the overall layout of the channels and the electrodes, as described above. An array of mechanical switches connected to conventional dc and ac power supplies controls the voltages at each of electrodes.

B. Fabrication Procedures

High resolution molding schemes enable fabrication of the necessary channel structures. Fig. 2 illustrates the process sequence, which is similar to that described by us in another publication [4]. It begins with photolithography to pattern a thick (~ 750 μm for the systems described here) layer of a

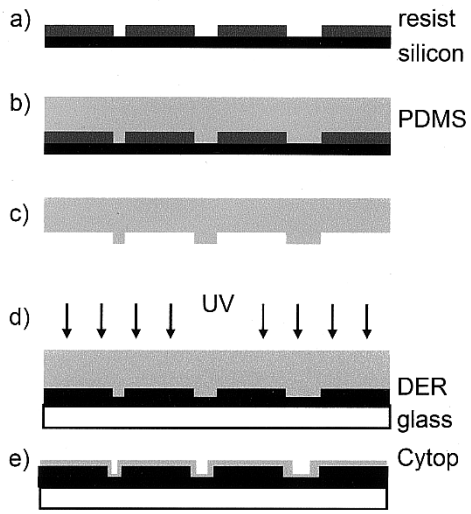

Fig. 2. Parts (a)–(e) illustrate the fabrication steps for producing molded microfluidic channels. Photolithography with a thick negative photoresist on a silicon wafer defines a 'master' structure, as illustrated in (a). Casting and curing a prepolymer to the elastomer poly(dimethylsiloxane) (PDMS) against this master (b) produces a mold with relief features in the geometry of the master, as shown in (c). This PDMS mold is placed against a layer of a photocurable epoxy (DER) on a glass slide, as indicated in (d). Passing ultraviolet (UV) light through the transparent PDMS mold cures the DER. Removing the mold completes the fabrication of the plastic channel structure. Dip coating (e) in a solution of a fluoropolymer (Cytop) produces a highly hydrophobic surface, which facilitates pinning-free fluid flow.

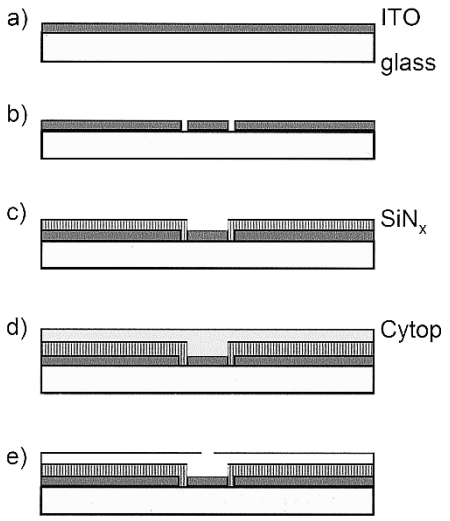

Fig. 3. Fabrication of the electrodes for the electrowetting pump begins with a glass slide (a) coated with indium tin oxide (ITO; 100 nm thick) that is then photolitographically patterned and etched with concentrated HCl to define the electrodes, shown in (b). Plasma enhanced chemical vapor deposition forms a uniform, 1-μm-thick dielectric layer of silicon nitride (SiN_x). Photolithography and reactive ion etching defines openings in the SiN_x that expose the ground electrodes in the electrowetting pumps. The resulting structure is illustrated in (c). Spin coating a 1-μm-thick layer (d) of a fluoropolymer (Cytop) creates the hydrophobic surface needed for fluid flow. A via hole is mechanically scratched through the Cytop layer to expose the ground electrodes. The final structure is shown in (e).

negative resist (SU-8 2075; Microchem Corp.) on a silicon wafer. Exposing the resulting structure to a vapor of tridecafluoro-(1,1,2,2,tetrahydrooctyl)-1-trichlorosilane (UCT, Inc.) forms a fluorinated silane monolayer on the exposed native SiO_2 layer. Casting and curing a prepolymer to the elastomer poly(dimethylsiloxane) (PDMS; Sylard 184, Dow Chemical) against this "master" structure forms a reusable mold with relief features in the geometry of the photolithographically patterned resist. The fluorinated monolayer prevents adhesion of the PDMS to the "master." Casting a thick ($\sim$800–1000 μm) layer of a photocurable epoxy resin (DER; Dow Chemical) on a glass slide, and then bringing the mold into contact with this layer causes the epoxy to flow and conform to the features of relief on the mold. Exposing the epoxy to ultraviolet light either through the transparent PDMS mold or through the glass substrate cures the polymer. Peeling the mold away completes the fabrication of the microfluidic channel structure. Dip coating in a fluoropolymer solution (Cytop; Asahi Glass) forms a highly hydrophobic surface that facilitates pinning-free fluid flow.

Fig. 3 shows the fabrication sequence for the electrowetting substrate. Photolithography and etching with concentrated HCl define the electrode pattern in a layer of indium tin oxide (ITO) on a glass plate. The bottom right inset to Fig. 1(b) shows the layout of the electrodes. Plasma enhanced chemical vapor deposition (Plasmatherm 760) forms a uniform dielectric of SiN_x ($\sim$1 μm thick) on top of this substrate. Patterned reactive ion etching removes this dielectric from common ground electrode. Spin coating a thin ($\sim$1 μm) uniform layer of Cytop onto this substrate creates the necessary hydrophobic surface. Although this layer does not itself provide a good dielectric, we often scratched this layer away from the ground electrode to make sure that there was good electrical contact with the conducting fluid plugs. We note that the nitride layer used here provides a much more robust and reliable dielectric than the spin cast polyimide implemented in previous work [3], [4].

We applied dc voltages of $\sim$100 V to the driving electrodes during testing. In some cases, we used ac signals with amplitudes of $\sim$50–80 V and dc offsets designed for RMS voltages of $\sim$100 V. This ac component was often useful to facilitate flow of the plugs over and around the optical fiber.

III. Results and Discussion

Fig. 4(a) shows an angled view image of a typical "master" for generating the molds that we used to build the microchannel structures. The fiber rests in the horizontal slot that runs roughly through the middle of this image. The recirculating channels are clearly visible; each contains a slightly widened region where the fiber passes through. The channels that allow micropipette loading of the conducting fluid plugs into these widened regions are oriented vertically; they terminate near the bottom edge of the image. Fig. 4(b) presents an angled view optical micrograph of the center region of three of the recirculating channels in an actual device. This image was collected by viewing the system from the top, through the transparent electrode substrate. The fiber is clearly visible. The electrodes appear as the faint areas aligned to the widened regions of the channels. The leads to these electrodes are visible as vertically oriented faint gray lines that extend to the bottom of this image.

By applying suitable voltages to the various electrodes, it is possible to control independently the positions of each of the eight conducting plugs. Fig. 5 shows top view optical micrographs of the system pumped to various configurations. A dark,

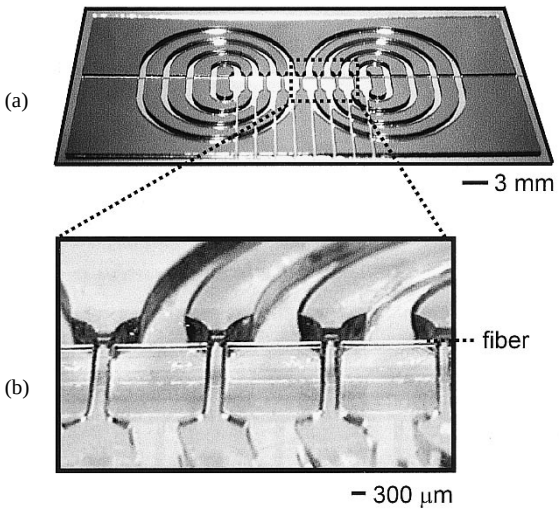

Fig. 4. Part (a) shows an image of the channel structure in photoresist on a silicon wafer. Part (b) presents an angled view optical micrograph of an unfilled device, which shows the channel structures and the position of the fiber. Faintly visible at the center of each channels is the ground electrode, which appears as a straight line.

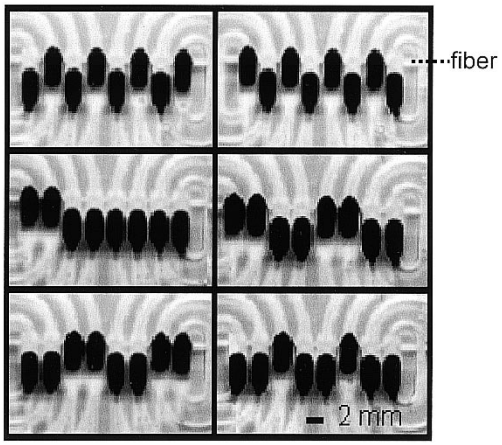

Fig. 5. Top views of a variety of different configurations obtained by independently moving each of the eight conductive fluid plugs (which appear as dark ovals) into or out of overlap with an optical fiber. The dotted line in the upper right frame illustrates the position of the fiber. The transparent plastic that forms the fluid channels is also visible.

water soluble dye was added to the conducting fluid plugs in order to enhance the contrast between them, the channels and the surrounding silicone lubricating fluid. The fiber rests horizonally, roughly at the center of each of these images. A portion of the recirculating channel structure is clearly visible. The plugs pump to one of two positions: up or down. In the up position, the plugs overlap the corresponding segment of optical fiber. In the down position, they are completely out of overlap. The plug movement stops naturally in each of these two positions, due to the use of patterned electrodes as virtual damns described previously. We note that obtaining complete overlap of the conducting fluid plug with the fiber can be challenging. The plugs have a tendency to flow over the fiber such that they contact only half of the outer surface of the fiber segment (the half that faces the electrode substrate). We found that it is possible to achieve complete overlap in a reliable manner by positioning

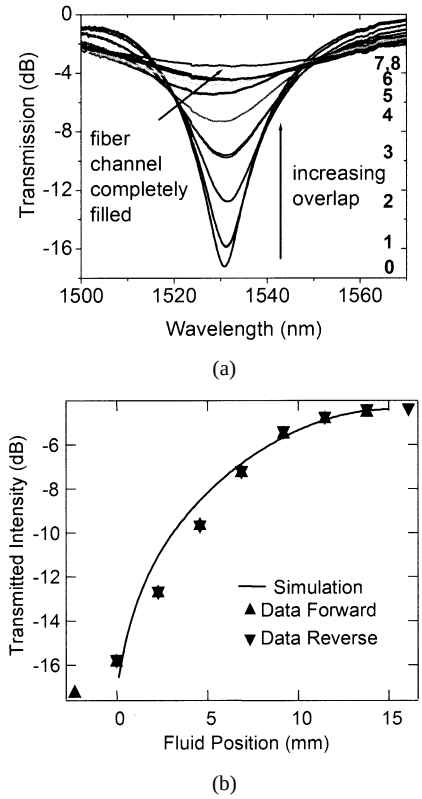

Fig. 6. Part (a) shows the transmission spectrum of a long period grating as eight index-matched plugs are pumped into overlap with the grating, sequentially starting with a plug at the edge of the grating. The spectra illustrate a discrete grating resonance for each plug configuration. The numbers on the right indicate the number of plugs that are in overlap. Part (b) (symbols) shows the depth of the center of the resonance as the plugs are pumped into (data forward) and out of (data reverse) overlap with the grating. The data show that the changes in the grating spectra are fully and digitally reversible. Also shown is the theoretically predicted behavior (solid line) for a grating comprising a segment of conventional LPG, and a section of a lossy LPG, for each plug configuration.

the fiber near the top of the channel structure and by applying a small ac component to the dc voltages that drive the electrowetting induced flow. Another challenge involves avoiding small drops of fluid that can remain on the fiber when a plug is driven out of overlap. These droplets can be largely eliminated by fluorinating the surface of the fiber using the hydrophobic silane monolayer chemistry described previously.

Arbitrary configurations of the plugs in the up and down positions are possible, as Fig. 5 suggests. We explored the use of this fluidic system for tuning the resonance feature associated with an LPG, whose attenuation spectra are determined both by the characteristics of the perturbation, and the index of the ambient. For measurements described here, we used a uniform 1.5-cm long LPG with a period of 362 μm (O/E Land, Inc.), which leads to coupling between the fundamental $\mathrm{LP}_{0,1}$ mode and the $\mathrm{LP}_{0,7}$ mode.

Fig. 6(a) shows transmission spectra recorded as the number of overlapping plugs increases from one to eight. It also presents a spectrum recorded in a separate experiment where the fiber was immersed completely in the conductive index matching fluid. The spectra reveal a systematic monotonic decrease in depth, without substantial shifts in center wavelength and without the introduction of additional structure

in the resonance. The existence of a diminished resonance upon the introduction of the fluid plug indicates that the fluid introduces loss in the cladding mode, thereby frustrating resonant coupling. In this experiment, the LPG monotonically decreases in strength because progressively larger segments of the grating are covered by the fluid plugs that serve to diminish the resonance. At any given plug configuration, two separate LPG's exist—one that is surrounded by air, and one that is covered by the fluid.

This system can be modeled by summing the contributions of the two gratings. This is justified whenever the two gratings do not interact resonantly—a condition experimentally confirmed by the absence of interference fringes in the grating spectra (see Fig. 6). The LPG in air has been extensively modeled in the past, and the coupling at resonance may be given by [5]

$$E_c = \sin(\kappa L) \tag{1}$$

where E_c is the electric field amplitude of the cladding mode, κ is the coupling coefficient of the LP, deduced from the strength of the LPG in air, and L is the length of the grating that remains surrounded by air. The LPG submerged in the fluid may be modeled by introducing an extra loss for the cladding mode evolution in the coupled mode equation. Since the fluid index is slightly higher than that of Silica, the cladding mode is not strictly guided. However, within the limited length of the grating, Fresnel reflections at the silica-fluid boundary permit the existence of a leaky (i.e., lossy) cladding mode [7]. The modified coupled mode equations for such a grating may be given by

$$\begin{aligned} \dot{E}_o &= i\delta E_o + i\kappa E_c \\ \dot{E}_c &= -i\delta E_c + i\kappa E_o - \alpha E_c \end{aligned} \tag{2}$$

where E_o is the electric field amplitude of the core mode, δ is the detuning parameter which is related to the spectral dependence of the grating, α is the loss in the cladding mode, and all other parameters were defined previously. The dots on top of E_o or E_c indicate differentiation with respect to z, the axis of propagation of light. Solving these equations yields the strength of the cladding mode at resonance, $\delta = 0$

$$\begin{aligned} E_c(L) &= \frac{-i\kappa}{\gamma} e^{\alpha L'/2}\left[e^{\alpha L'/2} - e^{-\alpha L'/2}\right] \\ \gamma &= \sqrt{\alpha^2 - 4\kappa^2} \end{aligned} \tag{3}$$

where L' designates the remaining length of the LPG that is covered by the fluid. Combining the contribution of the two gratings [(1) and (3)] yields the total cladding mode amplitude at the end of the LPG. From energy conservation, the core mode amplitude (light remaining in the fiber after passing through the LPG—the experimental measurand) can be deduced.

Fig. 6(b) shows the experimentally measured depth of the center position of the resonance for various numbers of plugs pumped into overlap. Also shown is the theoretical prediction deduced from (3). The two curves match fairly well, though some discrepancies exist in the mid points of the curve. This may be due to the fact that the modeled grating assumes continuous overlap of the fluid along the length of the grating, while the discrete nature of the plugs introduced 200 μm regions between each plug where no fluid is introduced. These existence of these spacers would also result in a resonance spectrum stronger than when the fluid completely covers the LPG, since the cumulative length of the *lossy* LPG would be shorter. This feature is evident in the spectra of Fig. 6(a).

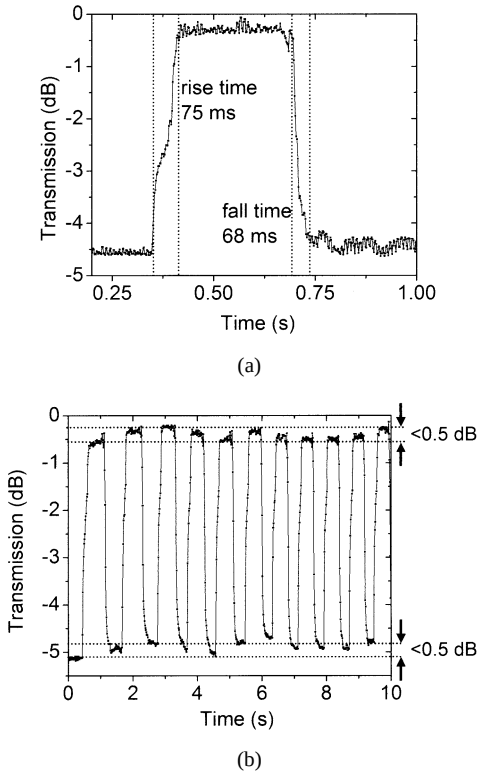

Fig. 7. Part (a) shows the time dependence of the change in transmission at a wavelength near the center of the grating resonance as a single plug is pumped into and out of overlap with the grating. The slight asymmetry of the on and off switching times is reproducible; it is related to the wetting dynamics of the fluid on the fiber. Part (a) shows multiple manually activated switching events. The on and off state transmission values are reproducible to <0.5 dB, which is comparable the noise in the measurement setup.

The data of Fig. 6(b) reveal a completely reversible transition, where different tuning states are achieved with a high degree of reproducibility. These data highlight an important benefit of the digital tuning approach. Fig. 7 illustrates another strength of the side pumped, multiple plug layout: relatively high speed operation. Part (a) shows the change in the transmission at a wavelength near the center of the LPG resonance as a function of time when a single plug is pumped into and out of overlap. The plug moves completely over the fiber in $\sim$75 ms; it moves completely out of overlap in $\sim$70 ms. Moving all plugs at once yields switching times that are within a factor of two of this single plug response. There is a short delay ($\sim$25–100 ms, depending on the position of the plug) between the time that the switch is activated and the time that the plug, which is initially slightly offset from the fiber, reaches the surface of the fiber and begins to modulate the transmission. The total switching speed (which might be considered to be the total time between switch activation and

complete fluid overlap) is still much faster for this system than it is for the devices use the single plug pumped along the length of the grating. This speed advantage increases in significance as the length of the fiber structure increases. Fig. 7(b) shows multiple manually triggered switching events using the plug that corresponds to the data in part (a). These results illustrate the digital operation of the device: to within uncertainties associated with our optical spectrum analyzer (~ 0.5 dB), the on and off states consistently yield the same transmission value.

IV. Conclusion

This paper introduces a new design for tunable microfluidic fiber (μFF) devices. It uses multiple plugs, each independently pumped back and forth by the electrowetting effect in a direction perpendicular to the axis of the fiber. Overlap of these plugs with a fiber structure (e.g., certain types of in-fiber gratings, fiber tapers, etched fibers, etc.) that is sensitive to fluid overlap alters its transmission characteristics in well defined ways. The resulting μFF devices offer digital operation with switching times that are significantly shorter than those of previous designs. The optical properties of the resulting tunable narrowband attenuator are good, and they are consistent with the ideal expected operation of the device. Independent control of the multiple plugs in these systems provides considerable flexibility in the type of tuning that can be achieved (i.e., phase shifted and superstructure gratings are possible). These and related approaches will be useful for adding tunability to other types of fiber structures as well as planar waveguides, photonic crystals and other components.

Acknowledgment

The authors would like to thank P. Mach and J. Hsieh for helpful discussions and advice.

References

[1] P. Mach, C. Kerbage, M. Dolinski, K. Baldwin, R. S. Windeler, B. J. Eggleton, and J. A. Rogers, "Tunable microfluidic optical fiber," *Appl. Phys. Lett.*, vol. 80, pp. 4294–4296, 2002.

[2] P. Mach, T. Krupenkine, S. Yang, and J. A. Rogers, "Dynamic tuning of optical waveguides with electrowetting pumps and recirculating fluid channels," *Appl. Phys. Lett.*, vol. 81, pp. 202–204, 2002.

[3] C. Kerbage, R. Windeler, B. J. Eggleton, P. Mach, M. Dolinski, and J. A. Rogers, "Tunable devices based on dynamic positioning of microfluids in microstructured optical fiber," *Opt. Commun.*, vol. 204, pp. 179–184, 2002.

[4] J. Hsieh, P. Mach, F. Cattaneo, S. Yang, T. Krupenkine, K. Baldwin, and J. A. Rogers, "Tunable microfluidic optical fiber devices based on molded plastic microchannels and electrowetting pumps," *IEEE Photon. Technol. Lett.*, vol. 15, pp. 81–83, 2003.

[5] A. M. Vengsarkar, P. J. Lemaire, J. B. Judkins, V. Bhatia, T. Ergodan, and J. E. Sipe, "Long period fiber gratings as band rejection filters," *J. Lightwave Technol.*, vol. 14, pp. 58–65, 1996.

[6] M. W. J. Prins, W. J. J. Welters, and J. W. Weekamp, "Fluid control in multichannel structures by electrocapillary pressure," *Science*, vol. 291, pp. 277–280, 2001.

[7] D. B. Stegall and T. Erdogan, "Leaky cladding mode propagation in long-period fiber grating devices," *IEEE Photon. Technol. Lett.*, vol. 11, pp. 343–345, 1999.

Francesco Cattaneo was born in Milan, Italy, in 1977. He was alumnus of Collegio Ghislieri (founded in 1567), Pavia, Italy. He received the diploma (laurea) *summa cum laude* in physics from the University of Pavia, Pavia, Italy, in 2001, where he realized an experimental setup to study the second harmonic generated, in reflection and in diffraction, by photonic crystals. From July–December 2002, he spent an internship at Bell-Labs working on microfluidic photonic systems. He is currently working toward the Ph.D. degree in physics at the University of Southampton, Southampton, U.K.

His research activity concerns photonic crystals.

Kirk Baldwin, photograph and biography not available at the time of publication.

Shu Yang, photograph and biography not available at the time of publication.

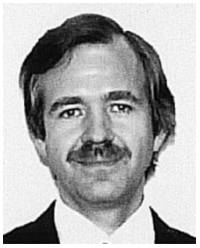

Tom Krupenkine received the Ph.D. degree in materials science from Moscow Institute for Physics and Engineering, Moscow, Russia, in 1992 and the Ph.D. degree in physics from Case Western Reserve University, Cleveland, OH, in 1996.

He joined Bell Laboratories, Lucent Technologies in 1998 after working for two years at Materials Research Laboratory, University of California, Santa Barbara. His current research is focused on physics of liquid–solid interaction, as well as on development of microfluidic devices for optical applications.

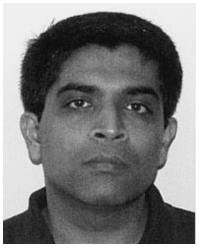

Siddharth Ramachandran received the Bachelor of Technology (B.Tech.) degree from the Indian Institute of Technology, Kanpur, in 1991, the M.S. degree from the University of Wisconsin, Madison, in 1993, and the Ph.D. degree in electrical engineering from the University of Illinois, Urbana, in 1998. His graduate work focused on the optical properties of chalcogenide glasses

Since November 1998, he has worked at Bell Laboratories, Lucent Technologies and subsequently OFS Laboratories, OFS-Fitel, first as a Member of Technical Staff, and since March 2003, as a Distinguished Member of Technical Staff. His research focuses on investigating fiber and fiber-grating devices in specialty dispersion-tailored fibers. He has authored 47 journal and conference publications, and is the editor of an upcoming book on dispersion compensation.

Dr. Ramachandran is a Member of IEEE-LEOS.

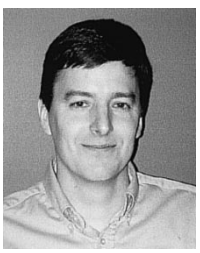

John A. Rogers received the B.A. and B.S. degrees in chemistry and physics from the University of Texas, Austin, in 1989. He received the S.M. degrees in physics and in chemistry in 1992, and the Ph.D. degree in physical chemistry in 1995, all from the Massachusetts Institute of Technology (MIT), Cambridge.

From 1995 to 1997, he was a member of the Harvard University Society of Fellows. He was with Bell Laboratories from 1997 through 2002, where he served as Member of Technical Staff and Director of Condensed Matter Physics Research. He is currently Professor in the Departments of Materials Science and Engineering and of Chemistry at the University of Illinois at Urbana/Champaign. His research interests include "soft" materials and patterning techniques for electronic and photonic systems.